Global Aerosol Climatology Project (GACP) Year 3 Report (Sept. 30, 2001)

PI: Thomas Charlock (1-757-864-5687; t.p.charlock@larc.nasa.gov)
Mail Stop 420, NASA Langley Research Center, Hampton VA 23681

Co-I: Wenying Su (w.su@larc.nasa.gov)
Mail Stop 420, NASA Langley Research Center/Hampton University, Hampton VA 23681

Collaborators: Zhonghai Jin (z.jin@larc.nasa.gov)
Fred G. Rose (f.g.rose@larc.nasa.gov),
David A. Rutan (d.a.rutan@larc.nasa.gov)
Ken Rutledge (c.k.rutledge@larc.nasa.gov)

http://snowdog.larc.nasa.gov/gacp/

Three topics in this report:

- Ocean BRDF (Boundary Conditions for GACP Retrieval)
- Chesapeake Lighthouse and Aircraft Experiment for Satellites (CLAMS)
- Year 2000 Aerosol Radiative Forcing at ARM SGP

Ocean BRDF (Boundary Conditions for GACP Retrieval)

The diffuse reflection of the sea (ocean reflection far displaced from the large specular reflection near the sunglint peak) is a crucial boundary condition for the retrieval of aerosol optical thickness (AOT) with AVHRR. GACP algorithms for this are based on the classic Cox-Munk formulations from the 1950s. The various EOS algorithms which will be used to validate more recent GACP retrievals with AVHRR alternately use both the diffuse reflection and the glint peak itself. Using special observations and theory, we have uncovered significant limitations to the Cox-Munk formulation. This component of our program has been headed by Dr. Wenying Su, who arrived at Langley in August 2000.

Observations of visible SW radiance reflected upward from the sea are made routinely with the Schulz SP1A Spectral Photometer. The rather expensive SP1A was purchased with GACP funds in Year 1 of GACP, after a thorough selection process, wherein it was noted as stable over the enormous dynamic range that is needed for ocean BRDF applications. A team led by Ken Rutledge deployed the SP1A at COVE (Cheaspeake Lighthouse), where it is collocated with a BSRN station (maintained by CERES), a Cimel photometer (GSFC AERONET), and standard meteorological and ocean wave measurements (NOAA).

In Fig. 1 below, Dr. Su compares radiance distributions measured using the SP1A with simulations using the 6S (Second Simulation of Satellite Signal in the Solar Spectrum) code (which uses Cox-Munk). The measured sunglint area is larger and more intense. The diffuse reflection (i.e., elevation vel of 10-60 deg and view azimuth vaz 90-150 deg in Fig. 1), which is used by AVHRR algorithms as a surface boundary condition for the retrieval of AOT.

Fig. 1 BRDF Measurements and Simulations

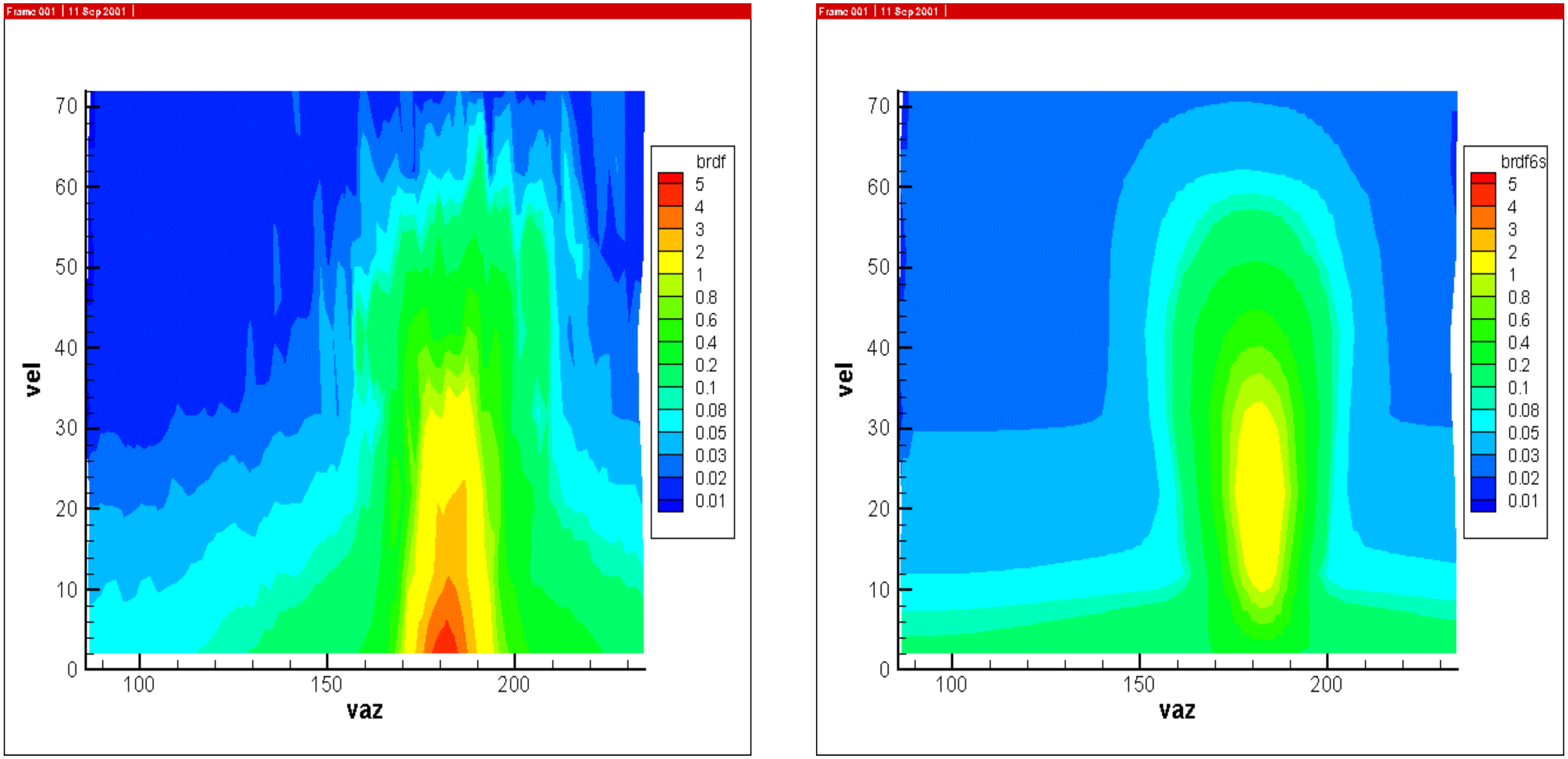

Comparison of observed and 6S simulated BRDF for 17 GMT (12 ET) for Jan. 10. Solar Zenith Angle is 58.8, Solar Azimuth Angle is 177.3. Aerosol optical depth is 0.033. Wind speed is 5.6 m/s and direction is 239.4.

When BRDF is examined at specular view zenith angles (Fig. 2), it can be normalized (not shown). We can then define RM as the ratio of maximum BRDF of the observation to simulation. The differences between the observed and simulated maximum BRDF increase with wind (Fig. 3); are larger for smaller viewing elevation angles; and are largest at neutral stability (same temperature for air and sea).

Specular Reflection

Fig. 2 Example of BRDF from theory (RED) and observation (GREEN). Note that observation is more strongly peaked.

RM Ratio of BRDF vs Wind

Fig. 3 Ratio RM (RED squares) of maximum BRDF of observation to simulation depends on wind speed (see GREEN line fit).

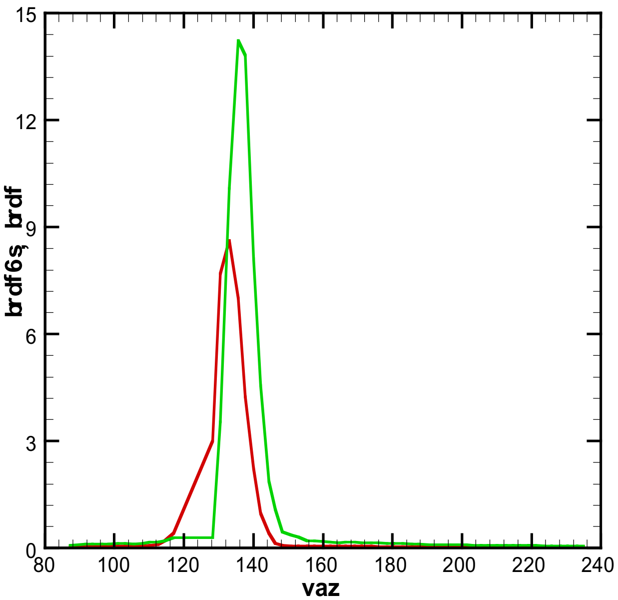

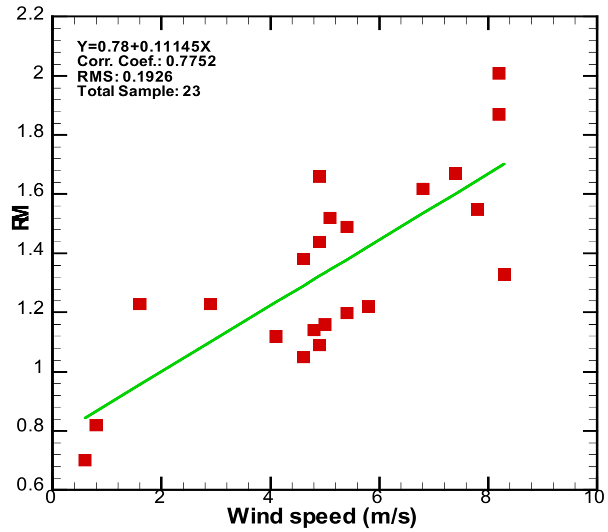

13:30GMT: Solar zenith angle is 78.2. BRDF

Dr. Su also participated in ACE-Asia by deploying the SP1A on bow tower of the RV Ron Brown in the Pacific (Spring 2001). Unfortunately, a night rogue wave smashed the equipment on the deck of the RV Brown! Measurements shown here were from the more extensive time series at the Lighthouse, where the SP1A continues to take data. See http://snowdog.larc.nasa.gov/gacp for journal manuscript.

Su, W., T. Charlock, and K. Rutledge, 2001a: "Preliminary Comparison of Theory and Observations for Radiance Emitted by the Ocean Surface at COVE", presentation at AGU Spring Meeting in Boston (May 2001).

Su, W., T. P. Charlock, and K. Rutledge 2001b: Observed reflectance distribution around sun glint at CERES Ocean Validation Experiment site. Journal manuscript. http://snowdog.larc.nasa.gov/gacp

Su, W., T. Charlock, and K. Rutledge, 2001c, "Comparison of Observations and Theory for Ocean Surface Reflectance during ACE-Asia and CLAMS", presentation for AGU Fall Meeting in San Francisco (Dec. 2001).

Chesapeake Lighthouse and Aircraft Experiment for Satellites (CLAMS)

CLAMS was a joint aircraft campaign involving CERES, MISR, MODIS, and GACP in the vicinity of the Chesapeake Lighthouse sea platform, July 10 to August 3, 2001. The original concept was a validation of CERES retrievals of broadband surface fluxes over ocean. By entraining resources from components of the MISR and MODIS teams with an interest in the remote sensing of aerosols, it was then possible to meet GACP objectives as well. The AERONET Cimel at the Chesapeake Lighthouse provides GACP with the only photometer measurement of AOT from a platform that is both rigid and over the open sea (i.e., high quality observations over the boundary condition where GACP operates). Collocated BSRN facilities enable a reliable diagnosis of aerosol radiative forcing – the key target for which GACP was formed. Similar surface observations of AOT are available at many sites; collocated observations of the surface reflectance are found at a very few. The specialized CLAMS aircraft observations provide a comprehensive description of the aerosols and ocean radiative boundary condition over several satellite pixels, rather than just the single fixed point of the Chesapeake Lighthouse (COVE). This enables a comprehensive test of the complete physics retrieving of aerosols and their radiative forcing with the MISR, MODIS, AVHRR, and CERES satellite sensors. CLAMS will validate the remote sensing of aerosols on EOS, which Dr. Mishchenko has indicated will in turn validate GACP.

For GACP, the University of Washington CV-580 was the most important aircraft in CLAMS. The CV-580 provided a suite of in situ sensors for aerosol size distribution and spectral optical properties, including PIXIE analysis for absorbing properties; the CAR (GSFC) for spectral BRDF of the surface; the AATS-14 (Ames airborne tracking sun photometer); and broadband radiative fluxes. The Langley OV-10 measured broadband and spectral SW fluxes (up and down) to establish the spatial representedness of the unique, long-term times series at COVE. Airborne spectral polarimeter observations (on a Cessna sponsored by GISS), an O2 A-band spectrometer (Learjet sponsored by Langley), and a FTS for humidity profiling (Perseus) complemented some of these measurements. The ER-2 flew with Air MISR and MAS.

CLAMS measurements were thorough, but for the most part, coastal. One truly unique CLAMS measurement was an overflight, in clear conditions, over an ocean buoy 250nm East of Cape May, N.J. : the dark, open ocean typically seen by AVHRR. The buoy provides surface winds, which are used by every model as a key determinant (along with spectral AOT itself) of ocean reflection. The CV-580 observed the ocean BRDF (CAR) and spectral AOT (AATS-14). Hence, the modeler has the tools to drive his BRDF model (i.e., as in Fig. 1 at COVE) and the observations to test the model, enabling closure for remote sensing boundary conditions at the ocean surface. This was capped by ER-2 highly intricate and directionally comprehensive measurements by Air MISR at 20km. This battery of Air MISR data constitutes a blue ocean virtual TOA satellite record of spectral radiances from a plethora of viewing angles. Algorithms can ingest this spectral “satellite” record, retrieve AOT, and compare with high quality observations for validation.

Dr. Zhonghai Jin has improved a model (Jin et al., 2001a, b) for computing the broadband surface albedo of the ocean which was observed in CLAMS and by COVE . To complement GACP, the PI encouraged the spectral application the sophisticated Jin-Stamnes coupled air-sea radiative transfer model, which simulates scattering and absorption in both the sea and the atmosphere explicitly (i.e., scattering by phytoplankton and a bottom of finite depth, as well as by atmospheric aerosols), rather than by treating one medium as a simple boundary condition for full radiative transfer in the other medium. Fig. 4 shows the theoretical ocean spectral albedo for 3 concentrations of chlorophyll, assuming the presence of air bubbles (and alternately, no bubbles) in the sea. Subtle deficiencies in diffuse scattering identified for 6S in Fig. 1, which are significant for sensing by GACP of the background aerosol, can be due to the unexpected presence of constituents such as bubbles.

Fig. 4 Modelled spectral albedo at 3 chlorophyll concentrations, with and without bubbles in the sea.

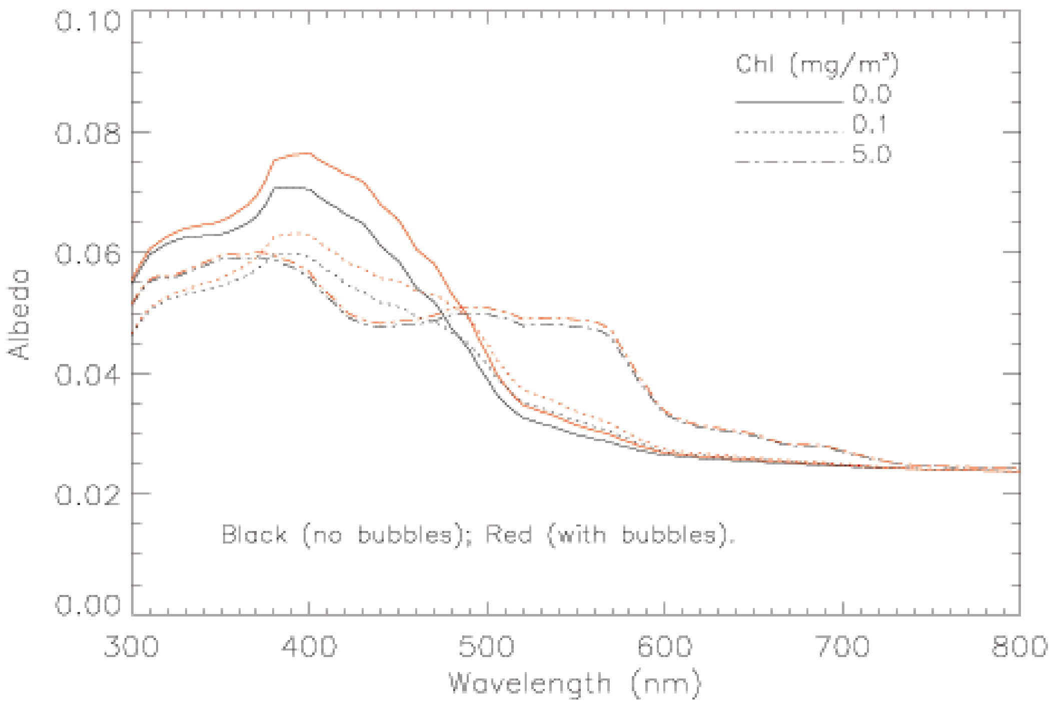

Jin et al. (2001b) made a detailed study of broadband sea albedo under clear skies at COVE for a full year. The computed broadband albedo in Fig. 5 included observed concentrations of chlorophyll, but not bubbles; more broadband albedo (and hence more scattering or less absorption) would be required to produce agreement with observations.

Fig. 5 Modelled and observed broadband albedo at Chesapeake Lighthouse

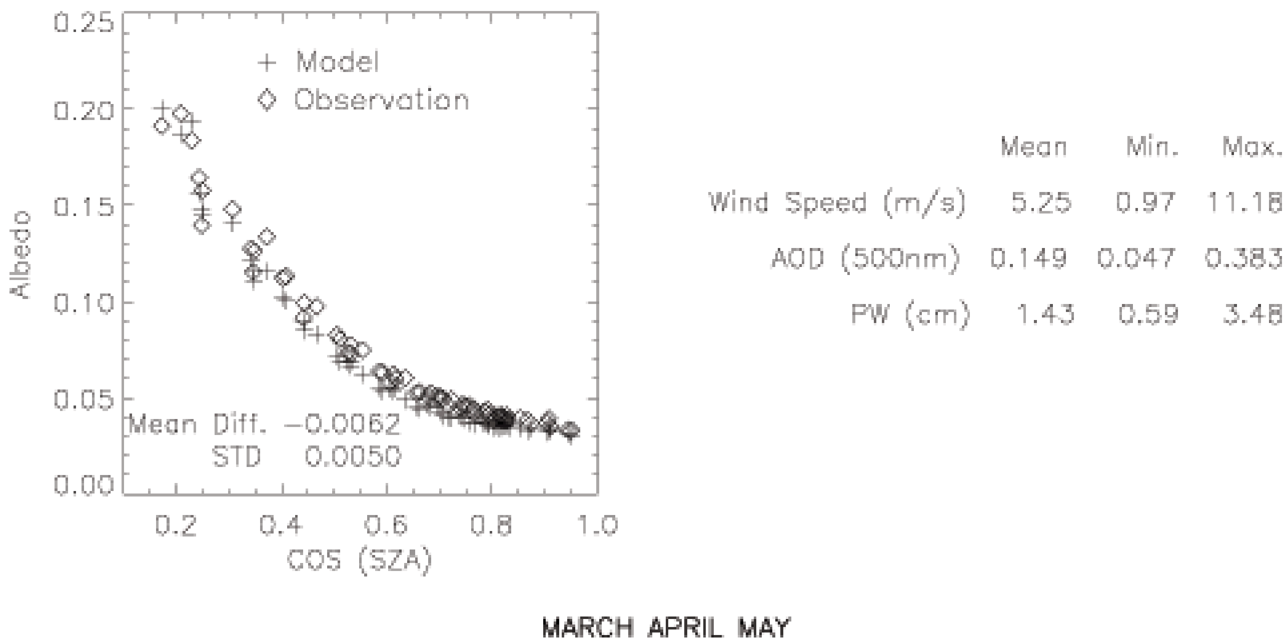

Deficiencies in the computed broadband albedo are also noted when comparing with the more comprehensive CLAMS aircraft data. In Fig. 6 below, the albedo from the rigid COVE platform is quite low in the morning because of shading by the platform; but the COVE albedo agrees with the aircraft during early afternoon, and the model does not.

Fig. 6 Sea albedo from COVE platform observations, OV-10 aircraft observations (RED) and Jin coupled MODEL versus time. Clear sky conditions at CLAMS 1200-2200 UTC on 17 July 2001.

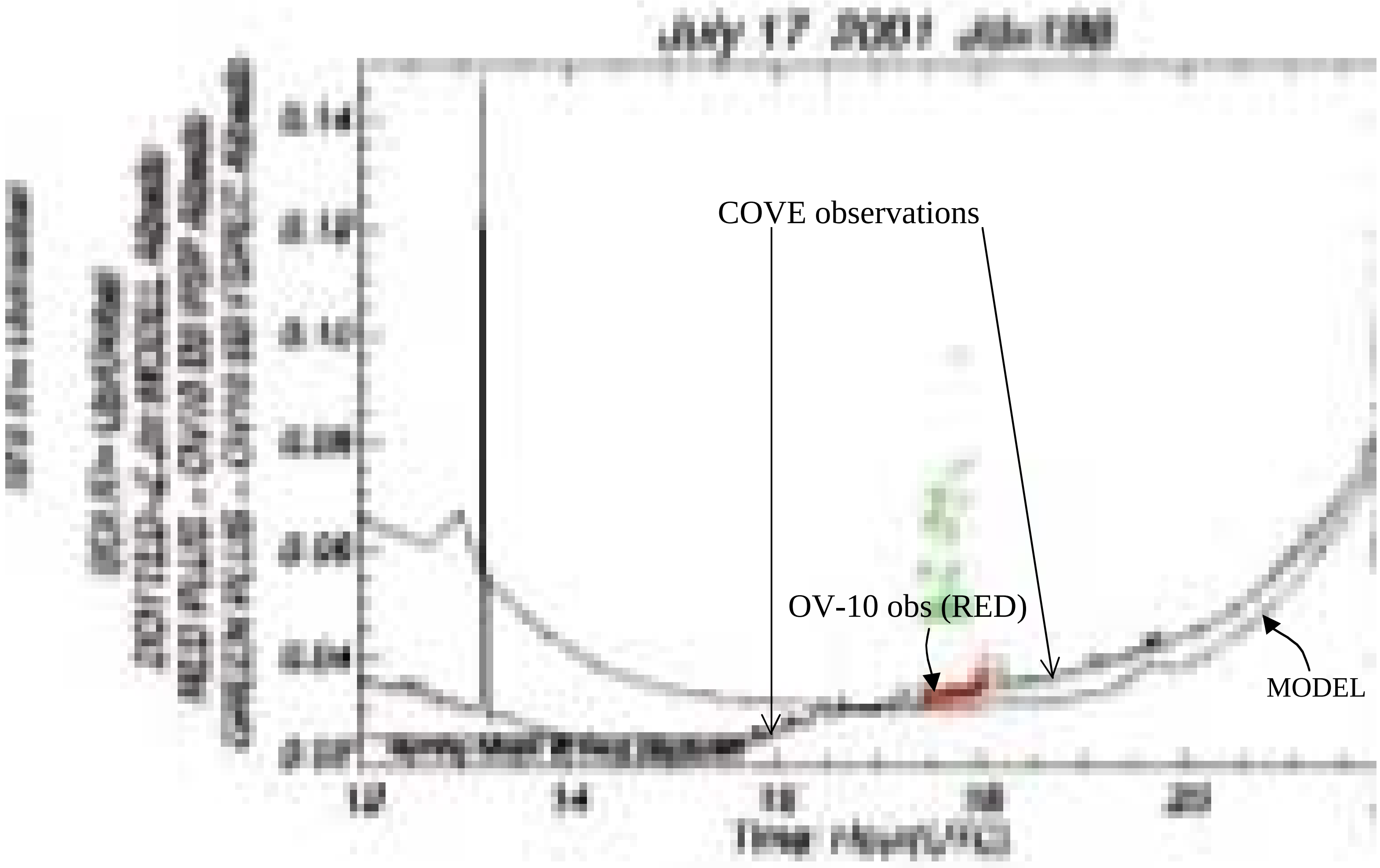

We conclude that from comparing observations and theory for narrowband radiances and broadband fluxes, reflection from the sea surface is not a solved problem. Further analysis of the huge CLAMS data set is needed to assure that all significant sea constituents are modeled satisfactorily. If we ignore this issue, the background AOT retrieved by GACP is liable to be a marker for our presently inadequate assumptions on the optical properties of the sea, rather than a faithful representation of nature.

Jin, Z., T. P. Charlock, and K. Rutledge, 2001: “Solar Radiation Measurements at the Chesapeake Bay COVE Site and Comparison With Model”, presentation at AGU Spring Meeting in Boston (May 2001).

Jin, Z., T. P. Charlock, and K. Rutledge, 2001: Analysis of broadband solar radiation and albedo over the ocean surface at COVE. Manuscript prepared for submission to J. O. A. T. (September 2001).

Year 2000 Aerosol Radiative Forcing at ARM SGP

Aerosols and the Residual Clear-sky Insolation Discrepancy

The "clear-sky insolation discrepancy" surfaced a few years ago: Several well-regarded theoretical simulations (sound radiative transfer codes and carefully measured inputs for them) produced values for clear sky shortwave (SW) insolation that exceeded measurements to 20-30 Wm-2. Now, by both carefully screening (Long-Ackerman) the radiometer observations and including the record of the newly installed Eppley Black and White (B&W) pyranometer, we find theory exceeding observations by means of –2.1 Wm-2 (total), -7.3 Wm-2 (direct horizontal), and 5.2 Wm-2 (diffuse) for 500 half-hourly observations during January-December 2000 at the SGP (Southern Great Plains) CF (Central Facility) C01 site. For moderate values of AOT, the aerosol forcing to surface insolation is considerably greater than the (now reduced) discrepancy of theory and observations.

[The reader may try his/her hand at these calculations. Input data is available for ARM SGP C01 and other sites at http://snowdog.larc.nasa.gov/gacp/ with a click to “CAVEHome”.]

The perspective from a detailed look at the time series is less rosy. The fine agreement in time mean for the direct horizontal, the component of flux which can be most confidently measured, is produced by compensation: Theory exceeds measurement for one period, and measurement exceeds theory for another. Results with permutations of Cimel versus MFRSR (Multifilter Rotating Shadowband Radiometer) for AOT (Aerosol Optical Thickness), the use of different broadband instruments, and confining to periods of agreement between duplicate measurements tell a similar story; and cannot be satisfactorily explained as due to minor H2O effects which were not in the present simulation. With the current generation of observations, we approach a limit for matching with simulations of the direct beam in an extended time series. This suggests that adjustments, for example, of soot fraction (here assumed 10% with a modified Fu-Liou code) to routinely assess aerosol absorption via comparison with the diffuse beam face the same barrier. The accurate assessment of anthropogenic forcing to the absorption of SW by the atmosphere yet remains beyond the grasp of climate science.

Table 1 shows the mean bias (model minus observation) and aerosol forcing (theoretical flux with AOT minus theoretical flux without AOT) at SGP during 2000. The advantage of the year 2000 is the installation of the Eppley B&W pyranometers for a more accurate diffuse and total SW flux at C01. For comparing the modeled and observed insolation, we have a sample of 500 intervals each of 30 minutes. The direct normal is the beam normal to the sun as observed by the Eppley Normal Incidence Pyrheliometer (PIR). Diffuse is measured by the shaded Eppley (offset corrected PSP at E13 or B&W at C01). The observed value for direct horiztonal is the mean of the minute-by-minute product of the direct normal and cosine of the solar zenith angle (SZA).

Table 1 Bias (Model-Obs) and Aerosol Forcing in Wm-2 at SGP during 2000

	Model - Obs		Sample	Aerosol
	E13	C01	N	Forcing
Surface				
Direct normal	-4.1	-10.0	500	-131.3
Diffuse	6.7	5.2	500	58.6
Total	3.3	-2.1	500	-27.5
Direct horizontal =(dir norm)*cosSZA	-3.4	-7.3	500	-86.1
TOA reflected	13.2	27.0	44	<-this N is tiny!

Figure 7 allows more careful examination of the differences of model minus observations for direct normal, diffuse (adjusted PSP for observations), total and direct horizontal SW at surface site E13 as time series. Each panel shows the mean difference of model and observations and the (standard deviation) in paretheses. While the differences for each component, such as –4.1 Wm-2 for the direct, are small for the annual mean, there is much scatter. The differences of model and observation are seen to vary considerably within a given (clear-sky) day. Further, there appear to be low frequency variations in the differences of model and observation. The bias for the diffuse at E13 is fairly small between days ~280-320 (second panel in Fig. 7).

Figure 7 Difference of model and observations (Fu-Liou model minus OBS) for broadband SW in Wm-2 versus time at ARM SGP site E13. Clear-sky data in half-hourly intervals. Panels display direct normal, diffuse (shaded PSP adjusted for thermal offset), total (sum of direct horizontal and diffuse), and direct horizontal (product of direct normal and cosSZA).

0301..ARM_SGP_E13 : CIMEL(7) SMOOTH AOTs: Jan2000-Dec2000 Cave Flux Data
Sonde T(z),Q(z): MWRPW : SMOBA O3(z) : CLEAR C.Long<0.02

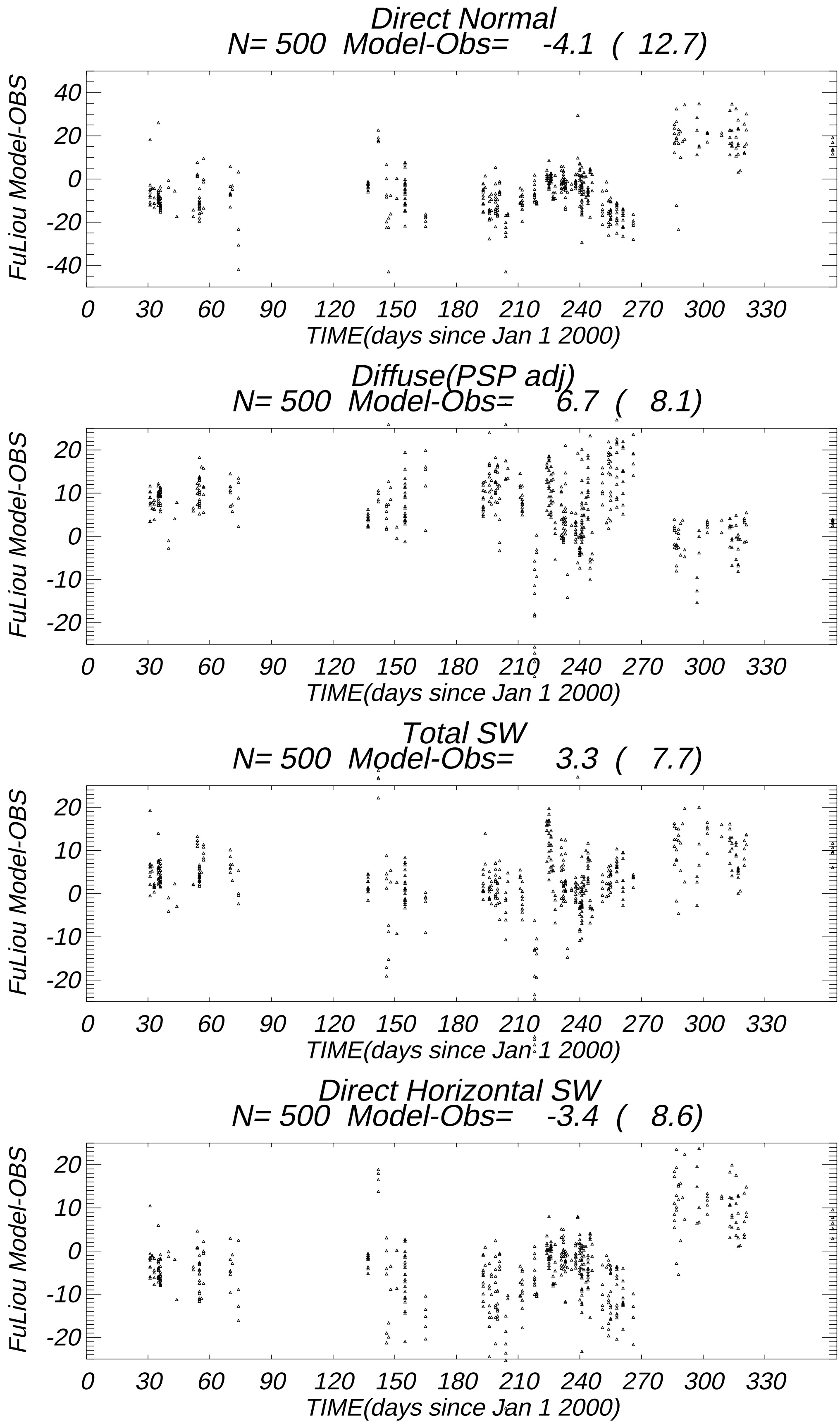

In Figure 8, the aerosol forcing is shown in red for site E13 as a scatter plot versus observed AOT. The forcing to total SW at the surface (third panels in Fig. 8) is linear with AOT. As a marker of the fidelity of the theoretical forcing (red), the scatter plots also depict the bias as model minus observation (black) versus AOT. For large values of AOT, the forcings have much larger absolute magnitudes than do the biases of model minus observation; this was also the case for the mean forcings and biases in Table 1. The forcings in Table 1 may be regarded as reliable estimates for the daylight mean, clear-sky direct aerosol forcing to the surface for year 2000 at the SGP CF. The modest success of this estimate is accompanied by the caveat that it is a result of our selection of 10% as the portion of soot in the computation. A 10% increase (decrease) in the percentage of soot would perturb the diffuse and total surface SW by roughly 10 Wm-2, and the resulting magnitude of the total surface forcing would no longer exceed that of the bias by a factor of 10. A further caveat is illustrated by the second panels of Fig. 8, wherein the bias (black marks) for diffuse flux shows a variation with AOT. For both the diffuse bias (second panel, black) and total bias (third panel, black) are slightly positive at low AOT and negative at high AOT. If the same plot is shown versus PW (not shown) rather than versus AOT, we find no such systematic variation of the bias with PW. This aspect of the bias for diffuse and total versus AOT would be consistent with an aerosol composition that has a larger fraction of soot at low AOT and a smaller fraction of soot at high AOT. Mlawer et al. (2000) also reported a case wherein more aerosol absorption was needed to establish closure at low AOT. While we have assumed a constant fraction of soot, the absorbing efficiency of the aerosol is consistent with a variable fraction of soot (or of some other absorber, such as large dust particles).

Charlock, T. P., F. G. Rose, and D. A. Rutan, 2001: Aerosols and the Residual Clear-Sky Insolation Discrepancy. Eleventh ARM Science Team Meeting Proceedings (Atlanta, 19-23 March 2001). 15 pp. See www.arm.gov under "Publications". Better version at http://snowdog.larc.nasa.gov/gacp/

Figure 8 Aerosol forcing (model with aerosol minus model without aerosol) in red and model bias (model with aerosol minus observations) in black for broadband SW in Wm-2 versus time at ARM SGP site E13.

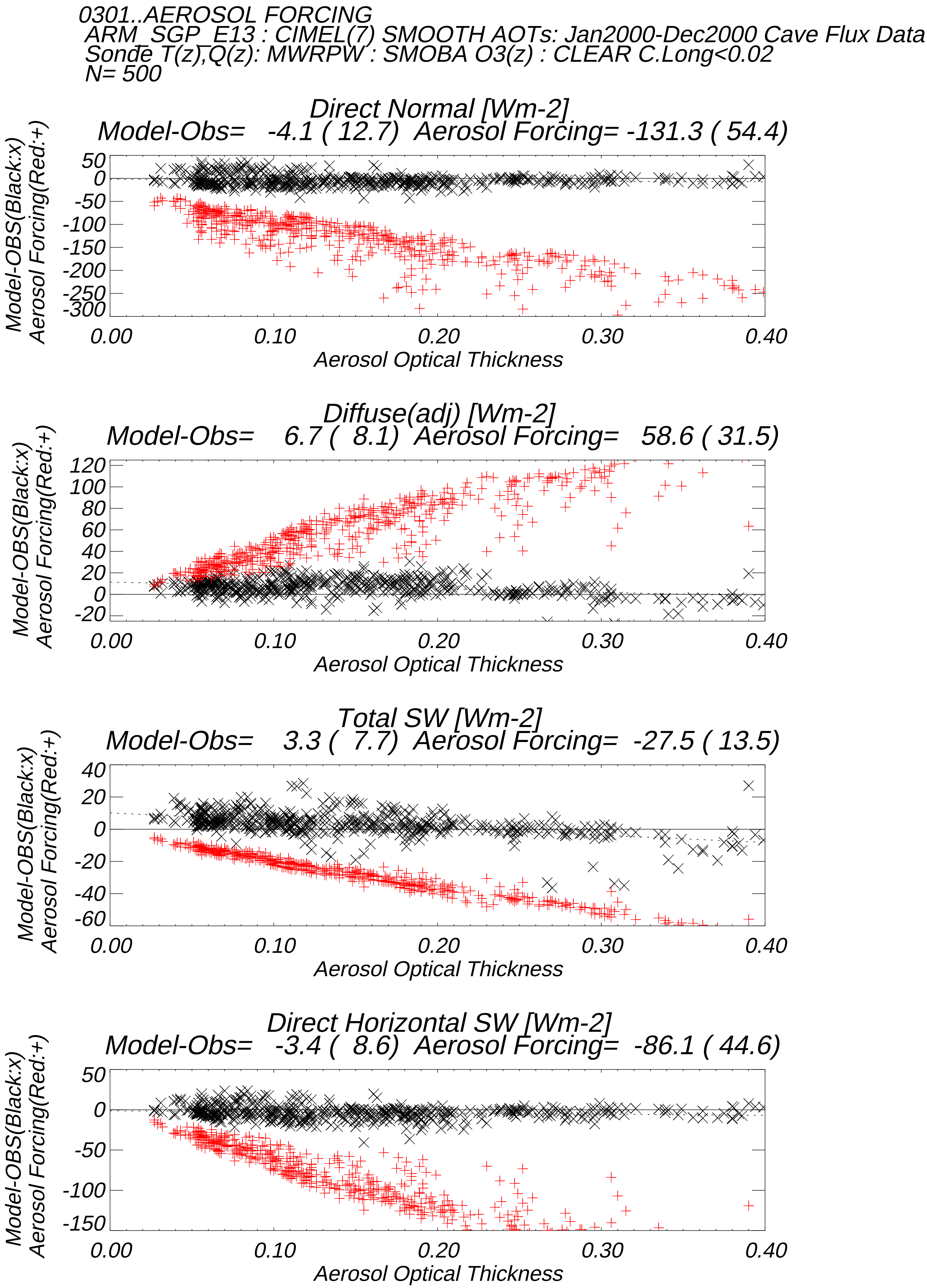
0301..AEROSOL FORCING
ARM_SGP_E13 : CIMEL(7) SMOOTH AOTs: Jan2000-Dec2000 Cave Flux Data
Sonde T(z),Q(z): MWRPW : SMOBA O3(z) : CLEAR C.Long<0.02
N= 500
Direct Normal [Wm-2]
Model-Obs= -4.1 (12.7) Aerosol Forcing= -131.3 (54.4)
Model-OBS(Black:x)
Aerosol Forcing(Red:+)
50
0
-50
-100
-150
-200
-250
-300
0.00
0.10
0.20
0.30
0.40
Aerosol Optical Thickness
Diffuse(adj) [Wm-2]
Model-Obs= 6.7 (8.1) Aerosol Forcing= 58.6 (31.5)
Model-OBS(Black:x)
Aerosol Forcing(Red:+)
120
100
80
60
40
20
0
-20
0.00
0.10
0.20
0.30
0.40
Aerosol Optical Thickness
Total SW [Wm-2]
Model-Obs= 3.3 (7.7) Aerosol Forcing= -27.5 (13.5)
Model-OBS(Black:x)
Aerosol Forcing(Red:+)
40
20
0
-20
-40
-60
0.00
0.10
0.20
0.30
0.40
Aerosol Optical Thickness
Direct Horizontal SW [Wm-2]
Model-Obs= -3.4 (8.6) Aerosol Forcing= -86.1 (44.6)
Model-OBS(Black:x)
Aerosol Forcing(Red:+)
50
0
-50
-100
-150
0.00
0.10
0.20
0.30
0.40
Aerosol Optical Thickness

The radiative transfer calculations in the above section were done by Fred G. Rose with a version of the Fu-Liou code. The input testbed ("CAVE" at www-cave.larc.nasa.gov/cave/) is managed by David A. Rutan.